Ion Mobility and Surface Collisions: Submicrometer Capillaries Can Produce Native-like Protein Complexes

Erin M. Panczyk,[‡] Joshua D. Gilbert,[‡] Gargi S. Jagdale, Alyssa Q. Stiving, Lane A. Baker, and Vicki H. Wysocki*

Cite This: https://dx.doi.org/10.1021/acs.analchem.9b03666

Read Online

ACCESS | 📊 Metrics & More | 📖 Article Recommendations | 🆂🅸 Supporting Information

ABSTRACT: The use of submicrometer capillaries for nano-electrospray ionization of native proteins and protein complexes effectively reduces the number of nonspecific salt adducts to biological molecules, therefore increasing the apparent resolution of a mass spectrometer without any further instrument modifications or increased ion activation. However, the increased interaction between proteins and the surface of the capillary has been shown to promote protein expansion and therefore loss of native structure. Here, we compare the effect of micrometer and submicrometer sized capillaries on the native structures of the protein complexes streptavidin, concanavalin A, and C-reactive protein under charge reducing conditions. We observe that the use of submicrometer capillaries did not result in a significantly higher charge state distribution, indicative of expansion, when compared to micrometer sized capillaries for complexes in 100 mM ammonium acetate and 100 mM triethylammonium acetate and for streptavidin in 200 mM ammonium acetate with no charge reduction. Additionally, no significant differences in collision cross sections were observed using ion mobility mass spectrometry. Finally, the dissociation behaviors of protein complexes ionized using micrometer and submicrometer capillaries were compared to determine if any structural perturbation occurred during ionization. Protein complexes from both capillary sizes displayed similar surface-induced dissociation patterns at similar activation energies. The results suggest that submicrometer capillaries do not result in significant changes to protein complex structure under charge reducing conditions and may be used for native mass spectrometry experiments. Submicrometer capillaries can be used to resolve small mass differences of biological systems on a QTOF platform; however, a laser tip puller is required for pulling reproducible submicrometer capillaries, and disruption in spray due to clogging was observed for larger protein complexes.
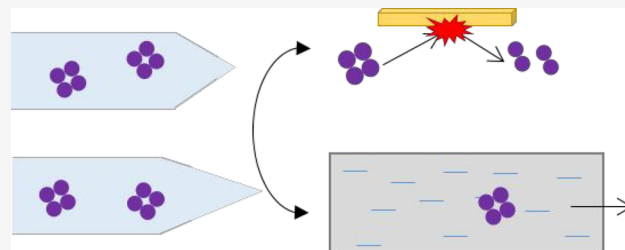
Native mass spectrometry has emerged as a powerful analytical technique, providing primary to quaternary structural information for proteins and protein complexes, and is complementary to traditional biophysical methods such as X-ray crystallography or NMR.[1,2] Specifically, native MS has been implemented to probe the stoichiometry and subunit connectivity of systems, including those deemed challenging by the previously mentioned methods due to the dynamic nature, heterogeneity, or low sample abundance of many protein complexes.[3,4] The rising use of native MS in structural biology has been made possible by the use of electrospray ionization (ESI), in which intact macromolecular complexes in solution can be ionized and transferred into the gas phase while maintaining noncovalent interactions.[5−7]

As previously described by Leney and Heck, the term "native", regarding MS, refers to the analyte solution conditions prior to ionization.[8] Solution conditions are chosen to preserve a native state by mimicking a physiological environment, through factors such as ionic strength and pH, while also using volatile electrolytes conducive to MS. The ionization of native protein complexes is widely believed to proceed via the charge residue model (CRM), in which

droplets undergo several evaporation events to dryness until the protein ion is released in the gas phase.[6,7] The presence of nonvolatile salts in electrospray solutions presents many challenges during the ionization process and is evident in the resulting mass spectra. Salts can form nonspecific adducts with the ionized protein complexes, limiting sensitivity, spectral resolution, and mass accuracy measurements, all of specific importance when probing any protein/protein or protein/ligand interactions.[9] To mitigate the effect of salt adduction, many researchers have employed the use of collisional activation or high source temperatures to remove nonspecific adducts. However, both methods increase the risk of unintentional complex activation and expansion or restructuring of protein complexes in addition to possible ligand loss,

therefore limiting the amount of native structural information that can be obtained.[10−12]

Recently, the use of submicrometer diameter (80−120 nm) emitters for nano ESI (nESI), without any additional instrument modifications, has been shown to significantly reduce the amount of salt adduction to proteins during MS analysis.[13−16] However, special attention must be paid when performing native MS experiments because submicrometer emitters have also been shown to supercharge proteins and possibly induce denaturation.[17,18] Mortensen and Williams have shown that proteins with a net positive charge in solution can interact with negatively charge silanol groups on the borosilicate capillary surface, resulting in surface-induced unfolding. They propose this effect is more pronounced with submicrometer capillaries due to the greater surface-to-volume ratio of smaller capillaries.[17] The desalting effect of submicrometer emitters will prove to be extremely beneficial for native MS experiments only if protein complex structure and ligand retention remain unperturbed during the ionization process. Here, we use two gas-phase techniques (ion mobility and surface-induced dissociation) to investigate if native-like protein complexes undergo the same silanol surface-mediated unfolding mechanism as previously observed for positively charged proteins.

Ion mobility spectrometry (IMS) and surface-induced dissociation (SID) are two gas-phase techniques employed here to characterize the effects of submicrometer diameter emitter ionization on protein complex native structure. Ion mobility is a gas-phase separation technique in which ions can be separated by their mass, charge, and shape; characteristics that influence their drift time through a weak electric field and buffer gas.[19,20] Drift tube ion mobility, specifically, can be used to directly calculate the gas-phase collision cross sections (CCS) of protein complexes without the use of calibrants to determine if the native state has been perturbed.[20−22] In this work, we compare CCS values obtained by spraying from submicrometer emitters and those traditionally used for native MS experiments (6−12 μm) to determine whether any structural rearrangement occurs.

Previous work in the Wysocki lab has shown that SID is a valuable activation technique to determine connectivity and stoichiometry of protein complexes.[23−27] SID consists of a single fast, high-energy collision and is capable of accessing higher-energy dissociation pathways often unattainable by multistep collision-induced dissociation (CID).[28−30] Additionally, SID has been shown to effectively probe protein restructuring by yielding different dissociation patterns for preactivated, structurally modified, versus native-like protein complexes.[31,32] The SID spectra of activated, restructured, or unfolded complexes tend to yield a greater abundance of highly charged monomer, similar to the fragmentation pattern obtained by CID. The SID spectrum for a native-like complex, on the other hand, has been shown to typically contain compact, higher-order oligomeric subunits with preferred cleavages indicative of smaller interfaces between subunits.[28,30,33] Differences in the abundances of varying oligomeric products at various SID energies, such as greater amounts of highly charged monomer as a result of expansion, are indicative of different protein complex structures. Here, the CCS values and relative abundances of SID products for a range of collision energies (energy resolved mass spectra, ERMS) are compared for submicrometer versus micrometer-sized emitters to investigate whether emitter-induced structural perturbations

limit the use of submicrometer capillaries for native MS applications.

■ EXPERIMENTAL SECTION

Static Nanoelectrospray Capillaries. Nanoelectrospray capillaries were produced using quartz glass capillaries with an inner diameter of 0.70 mm and outer diameter of 1.00 mm (Sutter Instrument Company, Novato, CA). The capillaries were pulled using a P-2000 Laser Based Micropipette Puller (Sutter Instruments, Novato, CA) for both micrometer and submicrometer sizes. The capillaries were imaged using a Quanta 600F scanning transmission electron microscope (Thermo Fisher Scientific, Hillsboro, OR) at the Nanoscale Characterization Facility at Indiana University (Department of Chemistry, Bloomington, IN), and capillary diameters were measured using ImageJ software (National Institutes of Health) (Figure 1). Submicrometer capillaries as used in this
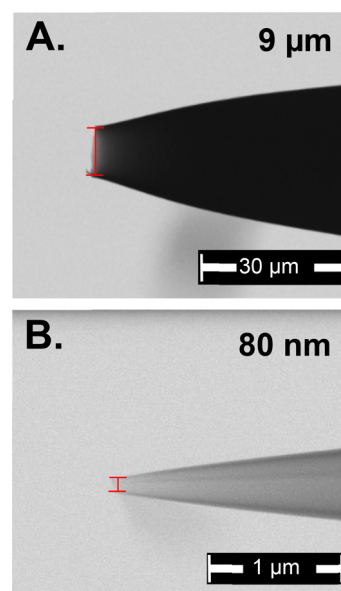
Figure 1. Scanning electron micrographs of (A) micrometer and (B) submicrometer quartz capillary tips used for experiments. Micrometer sized capillaries ranged from 6 to 12 μm in diameter, and submicrometer capillaries ranged from 80 to 120 nm in diameter.

work refer to those with pulled inner diameters ranging from 80 to 120 nm, and the micrometer-sized capillaries used throughout this work range from 6 to 12 μm in inner diameter. Flow rate approximations were performed using the difference in the mass method and determined to be 2.7 ± 0.9 nL/min for submicrometer and 1.8 ± 0.4 nL/min for micrometer capillaries (Table S1). For mass spectrometry experiments, ions were generated by bringing a platinum wire in contact with the analyte-containing solution in the back of the capillary opposite to the spray and applying 0.6 kV (submicrometer) and 1.1 kV (micrometer) potential to the capillary relative to the mass spectrometer entrance. A portion of the capillaries was imaged before and after electrospray experiments to ensure tip integrity (see Figure S1). The applied potentials were slowly ramped to obtain maximum ion signal while preventing any damage to the capillary opening through discharge events. Mass spectral evidence of submicrometer capillary damage at high electrospray voltage can be found in Figure S2.

Ion Mobility-Mass Spectrometry. All ion mobility experiments for CCS measurements were performed on a Waters Synapt G2 Q-IM-TOF (Wilmslow, UK) modified to include a 25 cm RF-confining (2.7 MHz and 150 V peak-to-peak amplitude) linear field drift cell in place of the standard Tri-Wave traveling wave ion mobility (TWIM) cell as described elsewhere ([Figure S3A](#)).[20,34] The potentials applied to the linear cell electrodes are decreased in constant values from the entrance to the exit of the cell. The drift voltage is defined as the difference between the entrance and exit electrode potentials and can be altered by changing the DC Offset and IM Bias values in the instrument software (MassLynx, Version 4.2). Drift time measurements were performed at ten different drift voltages ranging from 60 to 155 V in approximately 2 Torr of helium gas (ultrahigh purity, >99.999%), providing a drift cell field strength of 1.2 to 3.1 V cm^{-1} per unit pressure in Torr. The low-field limit for native-like protein complex ions such as those used here is much greater than that previously reported for peptide ions.[20] Pressure within the linear field drift cell was measured using a calibrated absolute pressure transducer (MKS Baratron model 626C, Wilmington, MA), and the temperature was measured using a thermocouple (Type K, ungrounded vacuum thermocouple, Omega Engineering, Norwalk, CT) placed directly inside the ion mobility cell within the vacuum chamber. The source temperature was set to 20 °C for all the experiments. CCS values were calculated using methods described previously.[35] Reduced mobility and therefore CCS values were determined from the slopes of the experimental drift times versus reciprocal drift voltage plots that yielded R^2 correlation coefficients of 0.99997 or greater ([Figure S4](#)). Plots were corrected for experimental temperature and pressure. Three technical replicates were performed on separate days for each protein complex for both micrometer and submicrometer capillaries and yielded CCS values with a % RSD < 0.55.

Surface-Induced Dissociation. All MS/MS experiments were performed on a Waters Synapt G2S (Wilmslow, UK) modified to perform SID as described elsewhere.[39] Briefly, the instrument was modified by shortening the trapping region to allow for installation of an SID device prior to the traveling wave ion mobility region ([Figure S3B](#)). Voltages were supplied to the SID device using a 10-channel external power supply and controlled by Tempus Tune software (Ardara Technologies, Ardara, PA). A single charge state was isolated for each protein complex using an extended m/z range quadrupole mass filter prior to the SID device. For SID experiments, the DC voltages applied to the front lenses of the device are tuned to direct ions into the surface, and the rear lenses are tuned to collect and transport the product ions to downstream optics. The acceleration voltage in SID is defined as the potential difference between the trap traveling wave ion guide exit and the surface. The trap traveling wave ion guide DC offset can be changed by adjusting the Trap Bias setting in the instrument software. SID lab frame collision energies (in eV) are defined as the acceleration voltage multiplied by the charge state of the precursor ion. For all experiments, the source temperature was set to 20 °C. After SID, product ions are separated by their mass, charge, and shape via traveling wave ion mobility prior to detection. Product ions of different oligomeric states are extracted from the mobility data and normalized to calculate their relative abundance. All mass spectrometer conditions were tuned to minimize inadvertent ion activation.

Materials. Ammonium acetate (AmAc), triethylammonium acetate (TEAA), and concanavalin A from jack bean (Con A) were purchased from Sigma-Aldrich (St. Louis, MO). Streptavidin from *Streptomyces avidinii* was purchased from Thermo Scientific Pierce Biotechnology (Rockford, IL). Recombinant C-reactive protein (CRP) produced in *E. coli* was purchased from Calbiochem (EMD Biosciences, Inc., San Diego, CA). Protein samples were buffer-exchanged into 200 mM AmAc (pH near neutral) with size exclusion chromatography spin columns (Micro Bio-Spin 6, Bio-Rad, Hercules, CA). For experiments on charge reduced proteins, a solution of 200 mM TEAA was added to the protein samples in a 1:1 (AmAc/TEAA) v/v ratio. Experiments on non-charge reduced protein complexes were performed in 200 mM AmAc only. The charge state distributions for streptavidin in 200 mM AmAc with only 20% TEAA were also measured and compared in the [Supporting Information](#). Final protein concentrations ranged from 3 to 5 μM.

■ RESULTS AND DISCUSSION

Charge State Distributions. The charge state distributions of protein complexes using nanoESI can be indicative of structural perturbation. Gas-phase unfolding of proteins can result in the exposure of basic sites, previously not accessible to solvent in the folded conformation, and unfolding can decrease or eliminate Coulombic repulsion. The exposure of additional basic sites can result in more charge retention on the protein complex during ionization, and different extents of unfolding can result in a higher charge state distribution. It should be noted that 20% v/v TEAA solutions are commonly used for native MS experiments; however, with submicrometer capillaries, a 50% v/v solution was required to obtain the same amount of charge reduction that we see with 20% TEAA and micrometer capillaries. For both size capillaries, final concentrations of 100 mM AmAc and 100 mM TEAA solutions were used. The mass spectra for streptavidin prepared with no TEAA and 20% TEAA can be found in [Figure S5](#). With the ionization of protein complexes proceeding via CRM, we have proposed two possible reasons for the need of higher TEAA concentrations with submicrometer capillaries: (1) The smaller capillaries produce smaller droplets with fewer TEAA molecules per protein. As a result, less charge reduction occurs during the desolvation process. (2) TEAA molecules are ejected from the surface of the droplet during desolvation events. Protein complexes will occupy the majority of the submicrometer droplets, thus exaggerating TEAA ejection due to increased charge repulsion at the droplet surface. The charge state distributions from micrometer and submicrometer capillaries for various protein complexes were analyzed, and the average charge states were compared. The full mass spectra for charge-reduced streptavidin are shown in [Figure 2](#) for the two capillary sizes. The full mass spectra for streptavidin without a charge-reducing reagent are included in [Figure S6](#). [Figure 2](#) shows that submicrometer capillaries do assist in desalting during the nanoESI process compared to micrometer capillaries as shown by an increase in the apparent resolution of the streptavidin mass spectrum. Streptavidin, as purchased from the manufacturer, contains some missed methionine cleavages on the individual monomers. As shown in [Figure 2](#), the presence of 3 methionine missed cleavages on the streptavidin tetramer can be resolved using the submicrometer capillaries on a Q-TOF platform. The stability of submicrometer capillaries to increase
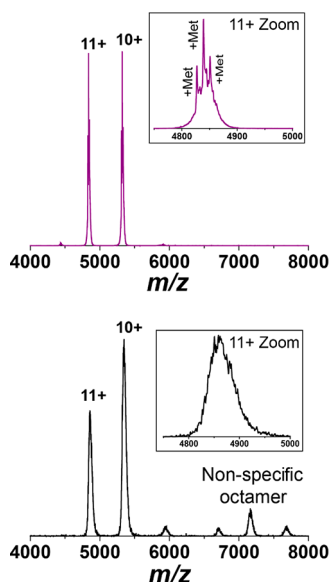
Figure 2. Full mass spectra for streptavidin in 100 mM AmAc and 100 mM TEAA for (top) a submicrometer capillary and a (bottom) micrometer capillary. A zoom-in of the 11+ charge state is shown. As purchased from the manufacturer, the streptavidin tetrameric complex may contain missed methionine cleavages on each monomer, as resolved in the submicrometer 11+ charge state.

the apparent resolution was also demonstrated over an hour of spraying (Figure S9). Additionally, due to the larger droplet sizes formed from the micrometer-sized capillaries, nonspecific octamer was observed in the resulting mass spectrum, suggesting the droplets are large enough to contain multiple protein complexes. The submicrometer capillaries are more likely to form droplets that contain only one protein complex per droplet as shown by the absence of any octamer formation. The full mass spectral data for Con A and CRP can be found in Figure S7.

Charge state distributions were calculated by normalizing peak areas and averaged for three replicates of both micrometer and submicrometer capillaries. The average charge states for various protein complexes are presented in Figure 3. While the average charge states obtained for protein complexes ionized via submicrometer capillaries are consistently slightly higher than those obtained for micrometer capillaries, and may be the result of differences in resolution associated with the two capillary sizes, the values are not significantly higher
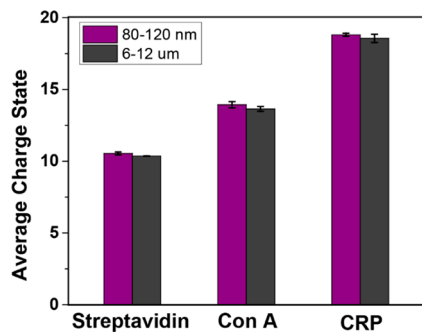

Figure 3. Comparison of average charge states for streptavidin, Con A, and CRP ionized with different size capillaries. Average charge states obtained from submicrometer capillaries are shown in purple and from micrometer capillaries, in gray.

(average charge states are within one standard deviation for both capillary sizes). Higher charge states would have been expected if expansion, unfolding, or supercharging was occurring during the ESI process.

Previous research has shown that submicrometer capillaries result in an increased electric field at the tip of the capillary, therefore producing droplets with a higher surface charge density, resulting in ions of higher charge states for peptides and small proteins.[16,17] During CRM ionization of protein complexes, low molecular weight charge carriers are also ejected from the droplets via the ion evaporation model (IEM). Here, we suggest that a higher percentage of the surface of larger protein complexes is more likely to reside at the interior of the droplet, as opposed to peptides or proteins. As a result, they are less sensitive to electrolyte ions that carry excess charge at the surface of the droplets, which may be ejected from the droplet during desolvation.[36,37] This process is likely exaggerated with even smaller capillaries as the protein complex will occupy the majority of the droplet, creating an even higher Coulombic repulsion at the droplet surface. Additionally, since experiments are being performed under native conditions and protein/protein interfaces bind the monomers to each other in the complex, we conclude the protein complexes retain an intact and compact quaternary structure, therefore limiting the available sites for protonation to only solvent accessible residues, which we expect to be similar for both capillaries. Further experiments with denatured protein complexes and submicrometer capillaries are necessary to determine if the compact structure of native protein complexes causes less sensitivity to the charge state in different size capillaries. Average charge state calculations showed no difference between proteins sprayed from the two different tip sizes; therefore, ion mobility and SID experiments were performed for further investigation.

Ion Mobility and CCS Measurements. Ion mobility measurements were performed for streptavidin, Con A, and CRP complexes. CCS values were calculated for multiple charge states using both micrometer and submicrometer capillaries. Structural perturbation using submicrometer capillaries, including collapse or expansion, should yield a significant decrease or increase in the CCS value, respectively.[38] The average CCS values for three protein complexes obtained using both micrometer and submicrometer capillaries are shown in Figure 4. The average CCS values for streptavidin and Con A, both tetrameric complexes, were not significantly different between capillary type ($p < 0.05$). CCS measurements were also performed for CRP, a cyclic pentamer known to collapse or expand depending on source or CID conditions, to determine if different complex geometries or sizes may behave differently during the ionization process using submicrometer capillaries. However, no significant difference was found in the average CCS values of CRP for different capillary sizes. Because the CCS values obtained with submicrometer capillaries did not significantly deviate from the values obtained with micrometer capillaries, it was concluded that no measurable structural expansion or collapse occurred during the ionization process. The CCS values for all complexes agree with previously measured values using a linear drift cell under charge-reducing conditions.[34]

Surface-Induced Dissociation ERMS. SID has been shown to be effective at probing disturbances to the native structure as reflected by changes in the abundances and charge state distributions of varying oligomeric products of dissoci-
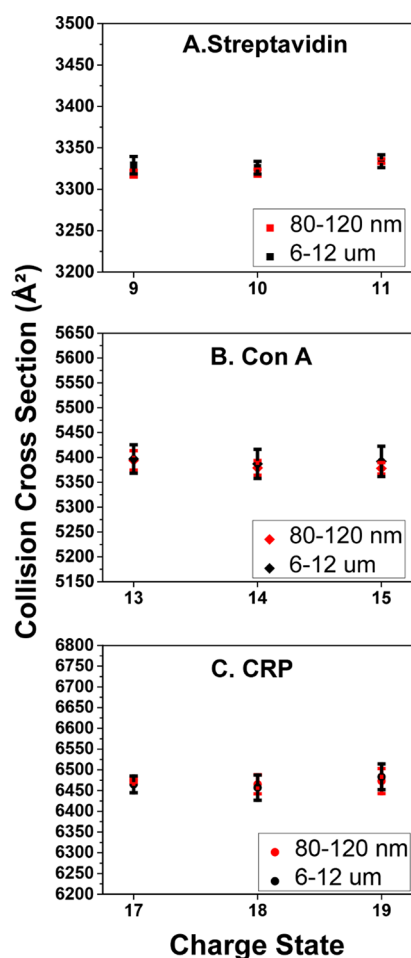
Figure 4. Average collision cross section measurements for various charge states of (A) streptavidin, (B) Con A, and (C) CRP using linear drift cell ion mobility spectrometry. Submicrometer capillary measurements are shown in red and micrometer capillary measurements are shown in black.

ation. Any subunit expansion or unfolding can result in more abundant monomer production at lower activation energies compared to a compact, native structure, as previously observed.[39] An example of the SID pathway for streptavidin (tetramer to dimer to monomer), along with the product ion spectra, can be found in Figure S8. Energy resolved mass spectra were acquired for streptavidin, Con A, and CRP complexes with both micrometer and submicrometer capillaries. Experiments were performed using a range of SID acceleration potentials starting from 30 to 60 V and extending to 150 V (kinetic energy of collision is charge state times acceleration voltage). The relative abundances of the dissociation products are displayed as a function of SID energy (Figure 5). Average crossing points and deviation were calculated by averaging each crossing point for the three individual replicates and determining one standard deviation from the mean energy value (Table 1). For submicrometer capillaries, the 11+ streptavidin tetramer to trimer, tetramer to monomer, and dimer to monomer crossing points are not significantly different from those obtained with micrometer capillaries (Figure 5A,B). However, a decrease in signal-to-noise was observed for data obtained with submicrometer capillaries, possibly leading to the higher variation for crossing point energies. For 13+ Con A, the differences in SID energy

observed for the tetramer to trimer, tetramer to dimer, tetramer to monomer, and trimer to monomer crossing points were within one standard deviation when comparing the two tip sizes (Figure 5C,D). Additionally, the relative abundances of the dissociation products remained consistent between tip sizes (Figure 5C,D). The use of submicrometer capillaries also did not result in significant changes for the 18+ CRP dimer to monomer crossing point or dissociation pattern (Figure 5E,F). For all protein complexes, no measurable structural change was detected using SID.

As previously mentioned, research groups have observed more extensive protein unfolding for species with a high net positive charge using submicrometer capillaries due to surface interactions with the negatively charged silanol groups on the capillary surface.[17] To ensure the charge-reducing agent was not interfering with or preventing unfolding events, SID experiments were also performed using streptavidin in 200 mM AmAc with no charge reducing agent. Figure 6 shows the ERMS data for the 14+ tetramer of streptavidin.

For non-charge reduced streptavidin, the crossing energies for tetramer to monomer and dimer to monomer are within one standard deviation of each other for both size tips, consistent with the results for charge-reduced streptavidin.

Less reproducibility from tip to tip for both IMS and SID experiments was observed for the micrometer sized capillaries. We propose this is likely due to greater variability in droplet sizes for the larger capillaries as compared to those generated by the submicrometer capillaries. Additionally, for larger protein complexes, such as CRP, the submicrometer capillaries were more prone to clogging, therefore limiting the time of analysis to roughly between 10 and 30 min per tip compared to micrometer capillaries that sprayed for over an hour. An example of the length of total ion chromatograms for the two tip sizes when spraying CRP can be found in Figure S10. It should also be noted that submicrometer capillaries result in a greater sensitivity when measuring protein complexes because total signal is not spread out over a broad, salt adducted peak. Because the applied spray voltage for submicrometer capillaries is lower (about 0.6 kV versus 1.0–1.2 kV for micrometer capillaries), we have observed that less sample solution is required compared to using larger capillaries. This is advantageous for protein complexes that are difficult to express or purify and only available in small quantities. An alternative technique that can be used for the desalting of protein complexes is rapid online buffer exchange, which has shown the ability to remove nonvolatiles from different buffer conditions.[40] However, submicrometer capillaries can be used when HPLC equipment is unavailable and if high throughput is not needed.

■ CONCLUSIONS

Charge state distributions, ion mobility CCS values, and SID ERMS measurements were compared for three protein complexes (streptavidin, Con A, and CRP), with ions generated by using nESI with micrometer and submicrometer capillaries to evaluate if submicrometer capillaries result in any measurable structural perturbation away from the native structure during the ionization process. The use of micrometer vs submicrometer capillaries does not result in significant differences in the average charge states of these three protein complexes, indicating no occurrence of major, measurable structural expansion or collapse. Linear field ion mobility was used to calculate the CCS for different charge states of the
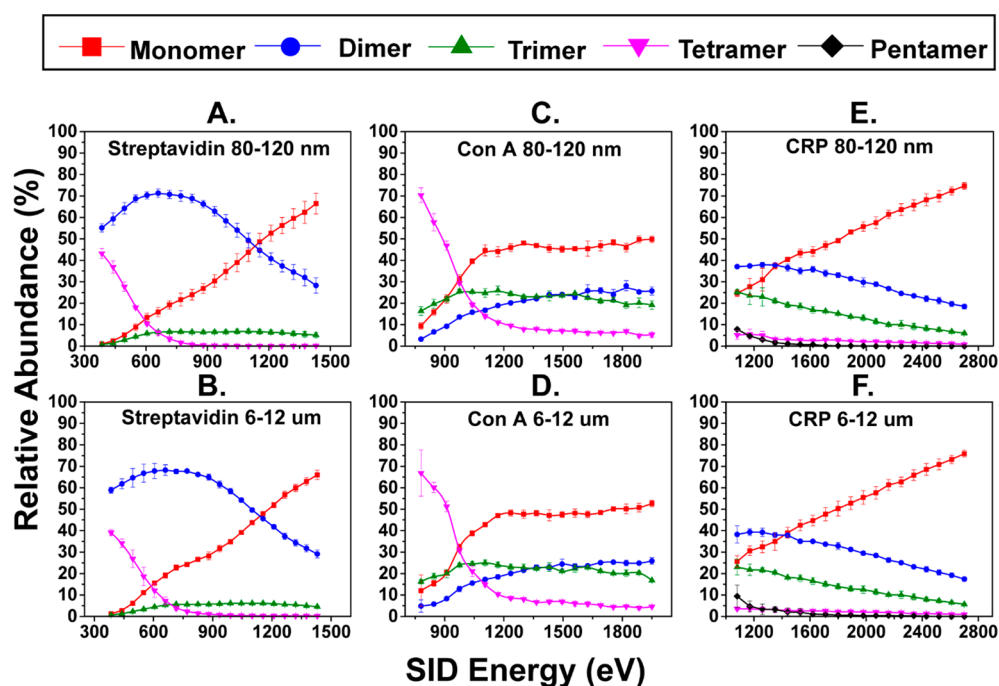
Figure 5. Energy resolved mass spectra (ERMS) of oligomeric product distribution (relative abundance as a function of SID energy). The ERMS plots are compared for submicrometer and micrometer sized capillaries of 11+ streptavidin tetramer (A, B), 13+ Con A tetramer (C, D), and 18+ CRP pentamer (E, F), respectively, in 100 mM AmAc and 100 mM TEAA solutions.

Table 1. SID Energies at Which Oligomeric Products Cross in Relative Abundance for ERMS Data Presented in Figure 5[a]

SID ERMS crossing point energies		
protein complex	tip diameter	
Streptavidin	80−120 nm	6−12 μm
tetramer → trimer	661.1 ± 25.1 eV	683.6 ± 14.7 eV
tetramer → monomer	592.6 ± 8.6 eV	585.3 ± 16.7 eV
dimer → monomer	1130.8 ± 43.0 eV	1139.8 ± 6.4 eV
Con A	80−120 nm	6−12 μm
tetramer → trimer	1000.8 ± 4.1 eV	1021.5 ± 18.4 eV
tetramer → dimer	1077.4 ± 13.8 eV	1085.7 ± 4.9 eV
tetramer → monomer	969.6 ± 6.5 eV	971.8 ± 2.7 eV
trimer → monomer	905.0 ± 27.1 eV	882.6 ± 58.4 eV
CRP	80−120 nm	6−12 μm
dimer → monomer	1371.7 ± 36.1 eV	1395.3 ± 62.9 eV

[a]Only products with crossing points in all three replicates are included.

three protein complexes. No discernible differences in CCS values were observed, further suggesting that no CCS measurable structural changes occurred using submicrometer capillaries vs micrometer capillaries. Finally, no tip-induced subunit expansion or collapse was observed on the basis of the dissociation patterns or crossing-point energies using SID ERMS under charge reducing conditions. When no charge reducing agent is added to the analyte solution, a similar SID behavior was demonstrated for streptavidin with both capillary sizes.

Results from these experiments demonstrate that there is no significant disruption of the measurable, native protein complex structure for two tetrameric and one pentameric complex using submicrometer capillaries for nanoESI under charge-reducing conditions. The use of submicrometer
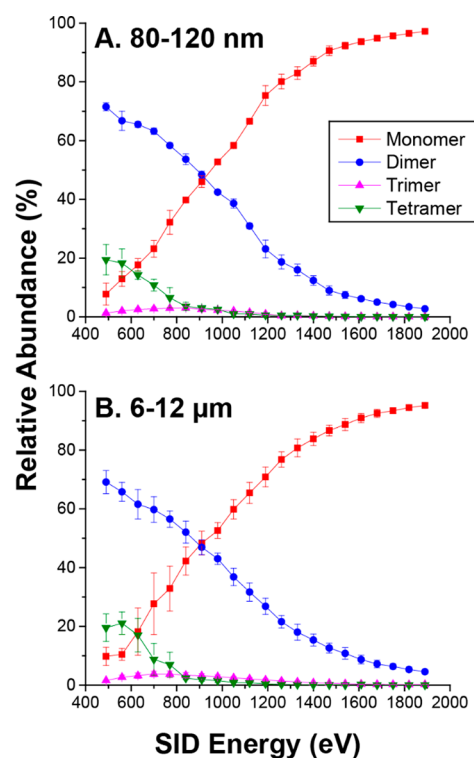
Figure 6. ERMS plots compared for 14+ streptavidin in 200 mM AmAc with no charge reducing agent using a submicrometer (A) and micrometer (B) capillary.

capillaries for native MS experiments is advantageous as desalting of the complexes can be achieved without complicated instrument modifications or use of activation techniques that may promote subunit restructuring. However, it should be noted that submicrometer capillaries do present

some challenges when analyzing large proteins or protein complexes. Specifically, the submicrometer tips more easily clog, disrupting spray stability and the length of analysis. Additionally, care must be taken to ensure that high spray voltages do not inadvertently damage the tip opening creating a larger tip diameter than expected. In this work and in previous studies, submicrometer capillaries increase the apparent resolution in native mass spectra, indicating that submicrometer capillaries may be implemented under charge reducing conditions for future work involving small mass difference protein modifications or ligand binding experiments.

■ ASSOCIATED CONTENT

ⓢ Supporting Information

The Supporting Information is available free of charge at https://pubs.acs.org/doi/10.1021/acs.analchem.9b03666.

> Flow rate measurements; images of capillaries before and after electrospray; mass spectra of streptavidin; instrument diagrams; example of drift time; full mass spectra; overview of the surface-induced dissociation device and example mass spectra; total ion current (PDF)

■ AUTHOR INFORMATION

Corresponding Author

Vicki H. Wysocki − *The Ohio State University, Columbus, Ohio;* ⓞ orcid.org/0000-0003-0495-2538; Phone: 614-292-8687; Email: wysocki.11@osu.edu
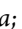
Other Authors

Erin M. Panczyk − *The Ohio State University, Columbus, Ohio;* ⓞ orcid.org/0000-0003-3779-6738

Joshua D. Gilbert − *The Ohio State University, Columbus, Ohio*

Gargi S. Jagdale − *Indiana University, Bloomington, Indiana*

Alyssa Q. Stiving − *The Ohio State University, Columbus, Ohio;* ⓞ orcid.org/0000-0002-9334-1212

Lane A. Baker − *Indiana University, Bloomington, Indiana;* ⓞ orcid.org/0000-0001-5127-507X

Complete contact information is available at:
https://pubs.acs.org/10.1021/acs.analchem.9b03666

Author Contributions

‡E.M.P. and J.D.G. contributed equally.

Notes

The authors declare no competing financial interest.

■ ACKNOWLEDGMENTS

■ REFERENCES

(1) Heck, A. J. R. *Nat. Methods* **2008**, *5* (11), 927−933.
(2) Liko, I.; Allison, T. M.; Hopper, J. T.; Robinson, C. V. *Curr. Opin. Struct. Biol.* **2016**, *40*, 136−144.
(3) van den Heuvel, R. H. H.; Heck, A. J. R. *Curr. Opin. Chem. Biol.* **2004**, *8* (5), 519−526.
(4) Sahasrabuddhe, A.; Hsia, Y.; Busch, F.; Sheffler, W.; King, N. P.; Baker, D.; Wysocki, V. H. *Proc. Natl. Acad. Sci. U. S. A.* **2018**, *115* (6), 1268−1273.
(5) Wilm, M. *Mol. Cell. Proteomics* **2011**, *10* (7), mcp.R111.009407.
(6) Konermann, L.; Ahadi, A.; Rodriguez, A. D.; Vahidi, S. *Anal. Chem.* **2013**, *85* (1), 2−9.
(7) Konermann, L.; Metwally, H.; Duez, Q.; Peters, I. *Analyst* **2019**, *144*, 6157−6171.
(8) Leney, A. C.; Heck, A. J. R. *J. Am. Soc. Mass Spectrom.* **2017**, *28* (1), 5−13.
(9) Konermann, L. *J. Am. Soc. Mass Spectrom.* **2017**, *28* (9), 1827−1835.
(10) Mirza, U. A.; Chait, B. T. *Int. J. Mass Spectrom. Ion Processes* **1997**, *162*, 173−181.
(11) Kitova, E. N.; El-Hawiet, A.; Schnier, P. D.; Klassen, J. S. *J. Am. Soc. Mass Spectrom.* **2012**, *23*, 431−441.
(12) Veenstra, T. D.; Tomilson, A. J.; Benson, L.; Kumar, R.; Naylor, S. *J. Am. Soc. Mass Spectrom.* **1998**, *9* (6), 580−584.
(13) Susa, A. C.; Xia, Z.; Williams, E. R. *Anal. Chem.* **2017**, *89* (5), 3116−3122.
(14) Xia, Z.; Williams, E. R. *J. Am. Soc. Mass Spectrom.* **2018**, *29* (1), 194−202.
(15) Xia, Z.; DeGrandchamp, J. B.; Williams, E. R. *Analyst* **2019**, *144*, 2565−2573.
(16) Yuill, E. M.; Sa, N.; Ray, S. J.; Hieftje, G. M.; Baker, L. A. *Anal. Chem.* **2013**, *85* (18), 8498−8502.
(17) Mortensen, D. N.; Williams, E. R. *Anal. Chem.* **2016**, *88* (19), 9662−9668.
(18) Mortensen, D. N.; Williams, E. R. *Analyst* **2016**, *141* (19), 5598−5606.
(19) Lanucara, F.; Holman, S. W.; Gray, C. J.; Eyers, C. E. *Nat. Chem.* **2014**, *6*, 281−294.
(20) Allen, S. J.; Giles, K.; Gilbert, T.; Bush, M. F. *Analyst* **2016**, *141*, 884−891.
(21) Lee, J. W.; Davidson, K. L.; Bush, M. F.; Kim, H. I. *Analyst* **2017**, *142*, 4289−4298.
(22) Laszlo, K. J.; Bush, M. F. *Anal. Chem.* **2017**, *89*, 7607−7614.
(23) Stiving, A. Q.; VanAernum, Z. L.; Busch, F.; Harvey, S. R.; Sarni, S. H.; Wysocki, V. H. *Anal. Chem.* **2019**, *91* (1), 190−209.
(24) Zhou, M.; Yan, J.; Romano, C. A.; Tebo, B. M.; Wysocki, V. H.; Paša-Tolić, L. *J. Am. Soc. Mass Spectrom.* **2018**, *29* (4), 723−733.
(25) Harvey, S. R.; Liu, Y.; Wysocki, V. H.; Laganowsky, A. *Chem. Commun.* **2017**, *53*, 3106−3109.
(26) Ma, X.; Loo, J. A.; Wysocki, V. H. *Int. J. Mass Spectrom.* **2015**, *377* (0), 201−204.
(27) Ma, X.; Zhou, M.; Wysocki, V. H. *J. Am. Soc. Mass Spectrom.* **2014**, *25*, 368−379.
(28) Zhou, M.; Wysocki, V. H. *Acc. Chem. Res.* **2014**, *47* (4), 1010−1018.
(29) Zhou, M.; Wysocki, V. H. *Acc. Chem. Res.* **2014**, *47*, 1010−1018.
(30) Wysocki, V. H.; Jones, C. M.; Galhena, A. S.; Blackwell, A. E. *J. Am. Soc. Mass Spectrom.* **2008**, *19* (7), 903−913.
(31) Quintyn, R. S.; Zhou, M.; Yan, J.; Wysocki, V. H. *Anal. Chem.* **2015**, *87* (23), 11879−11886.
(32) Harvey, S. R.; Yan, J.; Brown, J. M.; Hoyes, E.; Wysocki, V. H. *Anal. Chem.* **2016**, *88* (2), 1218−1221.
(33) Harvey, S. R.; Seffernick, J. T.; Quintyn, R. S.; Song, Y.; Ju, Y.; Yan, J.; Sahasrabudde, A. N.; Norris, A.; Zhou, M.; Behrman, E. J.; Lindert, S.; Wysocki, V. H. *Proc. Natl. Acad. Sci. U. S. A.* **2019**, *116* (17), 8143−8148.
(34) Stiving, A. Q.; Jones, B. J.; Ujma, J.; Giles, K.; Wysocki, V. H. Collision Cross Sections of Charge-Reduced Proteins and Protein

Complexes: A Database for CCS Calibration, submitted for publication.

(35) Bush, M. F.; Hall, Z.; Giles, K.; Hoyes, J.; Robinson, C. V.; Ruotolo, B. T. *Anal. Chem.* **2010**, *82*, 9557−9565.

(36) Hogan, C. J.; Carroll, J. A.; Rohrs, H. W.; Diswas, P.; Gross, M. L. *Anal. Chem.* **2009**, *81* (1), 369−377.

(37) Konermann, L.; Metwally, H.; Duez, Q.; Peters, I. *Analyst* **2019**, *144*, 6157.

(38) Quintyn, R. S.; Zhou, M.; Dagan, S.; Finke, J.; Wysocki, V. H. *Int. J. Ion Mobility Spectrom.* **2013**, *16* (2), 133−143.

(39) Zhou, M.; Huang, C.; Wysocki, V. H. *Anal. Chem.* **2012**, *84* (14), 6016−6023.

(40) VanAernum, Z.; Busch, F.; Jones, B. J.; Jia, M.; Chen, Z.; Boyken, S. E.; Sahasrabuddhe, A.; Baker, D.; Wysocki, V. Rapid Online Buffer Exchange: A Method for Screening of Proteins, Protein Complexes, and Cell Lysates by Native Mass Spectrometry. 2019, *ChemRxiv.org*. e-Print archive. DOI: 10.26434/chemrxiv.8792177.v1.